ELECTRON-CLOUD EFFECTS IN THE POSITRON LINACS OF FUTURE LINEAR COLLIDERS

A. Grudiev, D. Schulte, F. Zimmermann, CERN; K. Oide, KEK

Abstract

Inside the rf structures of positron (or electron) linacs for future linear colliders, electron multipacting may occur under the combined influence of the beam field and the electro-magnetic rf wave. The multipacting can lead to an electron-cloud build up along the bunch train. Electrons are also created by collisional and field ionization of the residual gas. We present simulation results of the electron build up for various proposed designs, and discuss possible consequences.

INTRODUCTION

Table 1 lists beam and rf parameters for the linacs of 3 different linear-collider projects. In the following, we discuss the primary-electron generation, electron accumulation and multipacting under the influence of beam and rf fields, as well as mechanisms of emittance degradation.

Table 1: Beam and RF cell parameters

design	TESLA	N(G)LC	CLIC
particles/bunch N_b [10^9]	20	7.5	4
bunch spacing L_{sep} [ns]	337	1.4	0.67
rms bunch length σ_z [μm]	300	110	35
initial energy E_b [GeV]	5	8	9
rms hor. size σ_x [μm]	260	57	14
rms vert. size σ_y [μm]	11	6	2
norm. h. emit. $\epsilon_{N;x}$ [μm]	8	3.6	0.55
norm. v. emit. $\epsilon_{N;y}$ [nm]	20	40	5
beta function $\beta_{x,y}$ [m]	80	14	5
pressure [ntorr]	10	10	10
frequency f_{rf} [GHz]	1.3	11.42	30
radius R [mm]	107	10.4	4
cell length L [mm]	115	7.5	3.3
rf wave length λ_{rf} [mm]	230	26	10
field E_0 [MV/m]	23.4	45.1	150

IONIZATION RATES

Primary electrons are created by ionization of the residual gas. The collisional ionization cross section σ_{ion} is abut 2 Mbarn for nitrogen or carbon monoxide molecules at utrarelativistic beam energies, yielding 6×10^{-8} electrons per meter and per positron for a pressure of 10 ntorr. Another ionization process that can become important in linear colliders is field ionization [1]. In the quasistatic limit, its ionization rate is [2, 3]

$$w = 4\omega_0 \left(\frac{E_i}{E_h}\right)^{5/2} \frac{E_a}{E} \exp\left[-\frac{2}{3}\left(\frac{E_i}{E_h}\right)^{3/2}\frac{E_a}{E}\right] , \quad (1)$$

where $\omega_0 = \alpha^2 m_e c^2/\hbar$ is the atomic frequency unit, E_h and E_i are the ionization potentials of hydrogen (13.6 eV) and the gas atom or molecule in question (11.26 eV

for carbon monoxide, 14.5 eV for nitrogen), and $E_a = m_e c^2 \alpha^4/(r_e e)$ is the atomic unit of the electric field. A different formula whose numerical evaluation yields similar results was given in [1]. The ionization probability is further enhanced at high frequencies [4], i.e., for short bunch lengths σ_z and large ionization energies E_i [3], namely at $E_i > e^2 E_0^2 \sigma_z^2/(4m_e c^2)$; the right-hand side is 24.1 eV for TESLA, 12.0 eV for NLC/GLC and 13.5 eV for CLIC. Field ionization may also occur for electron beams and could there enhance fast beam-ion instabilities. The probability of field ionization rises steeply from 0 to 1 at a field of about 20 GV/m. Such beam fields are expected at higher beam energies in CLIC and possibly in NLC/GLC. Assuming that, at 500 GeV/c, the beam is ionized within a few rms beam sizes, the ionization rate amounts to the production of several 10^7 electrons per meter and per passing bunch, which is some orders of magnitude more than from collisional ionization. The progress of field ionization over successive bunches depends on the thermal motion of molecules. At room temperature, the rms vertical distance travelled by a gas molecule between two successive bunches is about 0.3–1 σ_y for CLIC, and larger for the other designs.
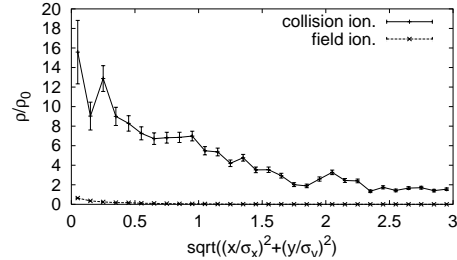
Figure 1: Electron density in units of local gas density as a function of the radial position in units of 0.1σ during a bunch passage at the end of the CLIC linac for collisional and field ionization.
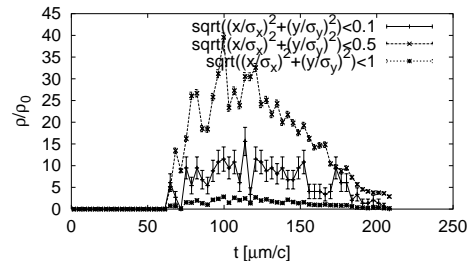
Figure 2: Average electron density, inside the 3 ellipses defined by $((x/\sigma_x)^2 + (y/\sigma_y)^2)^{1/2}$ equal to 0.1, 0.5 and 1, in units of the local gas density as a function of time during the passage of a CLIC bunch with field ionization.

Figure 1 shows the radial distribution of electrons during a bunch passage at the end of the CLIC linac. The com-

bined effect of electron creation by ionization and pinch near the bunch center is evident. Electrons inside the bunch perform 1–2 oscillations in the beam potential at the start of the linac and about 3 times more at its end, for all 3 projects. In the case of collisional ionization the peak electron density in Fig. 1 is about 70% of the local gas density, which, at 10 ntorr, is 3×10^{14} m^{-3}. With field ionization, the electron density is about 15 times higher than the gas density. Figure 2 illustrates the time evolution along the bunch of the central electron density with field ionization.

ELECTRON BUILD UP

The electrons are subjected to the field of the beam and to the electric and magnetic fields of the rf. The peak electric field of the rf becomes comparable to the peak field of the beam at a transverse distance $r_{\mathrm{crit}} \approx 2 N_b r_e m_e c^2 / \left(\sqrt{2\pi} \sigma_z (e E_0) \right)$, which is about 1/2–1/3 of the iris radius for GLC/NLC and CLIC, and 1/10 of the iris radius for TESLA. Therefore, the beam field appears important during the creation of the electrons and the initial acceleration close to the beam, but not for the electron motion at larger amplitudes. An electron starting from rest, during half an rf cycle passes a longitudinal distance

$$\Delta z \approx \int_0^{T_{\mathrm{rf}}/2} \sqrt{\frac{\frac{e^2 E_0^2}{\omega_{\mathrm{rf}}^2}(1 - \cos \omega_{\mathrm{rf}} t)^2}{m_e^2 + \frac{e^2 E_0^2}{\omega_{\mathrm{rf}}^2 c^2}(1 - \cos \omega_{\mathrm{rf}} t)^2}} \, dt \, , \quad (2)$$

which amounts to 0.08 m, 4 mm, and 2 mm for TESLA, GLC/JLC and CLIC, respectively. These distances are a significant fraction of the cell lengths in Table 1. The maximum energy gain in half an rf cycle is

$$\Delta E \approx \sqrt{\left(\frac{e E_0 c}{\pi f_{\mathrm{rf}}}\right)^2 + m_e^2 c^4} - m_e c^2 \, , \quad (3)$$

or 1.3 MeV, 120 keV, and 190 keV for TESLA, NLC/GLC and CLIC, respectively.

The primary ionization electrons are either trapped near the centre of the chamber by the beam field and rf fields, possibly accelerated in the longitudinal direction, or they escape radially towards the wall, where they can induce multipacting. The electron cloud build up is modeled by a modified version of the code ECLOUD. It is important to use a sufficient number of time steps (typically several 1000 between bunches) in order to avoid spurious multipacting: a position error of 1 μm, with an rf field of 200 MV/m yields an electron energy of 200 eV, close to the maximum of the secondary emission yield.

To obtain a realistic description of the rf forces acting on the electrons, a 'snapshot' of the complex amplitudes for the longitudinal and radial electric field and the azimuthal magnetic field of the rf inside a CLIC cell as function of the radial and longitudinal coordinates were computed by HFSS. These fields are read into the ECLOUD code. Depending on the longitudinal position at the moment of its creation during a bunch passage, a complex phase factor is determined for each individual electron, such that the local rf phase is correctly synchronized with the bunch arrival. If

an electron moves longitudinally the time relation between the rf wave and the beam forces of later bunches will dephase from the exact value. This is difficult to avoid in the present version of ECLOUD, where the bunch arrives 'everywhere in z' at the same time. The present aproximation is valid, if the beam field is important primarily after the electron creation inside or near the bunch, while at later times, when the electrons reside at larger amplitudes, the rf fields dominate. The phases of the rf field are kept synchronized with the electron motion throughout the simulation. The rf force on an electron is obtained by linear interpolation between the field values on the grid points computed by HFSS. The beam force is computed as for free space. A boundary with iris was introduced at either end of the cell, such that electrons are lost and produce secondaries when they impact on this boundary. At the opening of the iris quasi-periodic boundaries are applied with an appropriate shift in rf phase of 120 degrees per cell length, so that, e.g., electrons leaving the cell at large z are re-injected at $z = 0$ with a proper shift in their complex phase factor. For the other projects we scaled all dimensions of the CLIC cell with the inverse of the rf frequency and adjusted the gradient to the target value. This does not represent the exact fields in the TESLA or GLC/NLC rf structures, but may reveal the dependence on frequency and gradient.
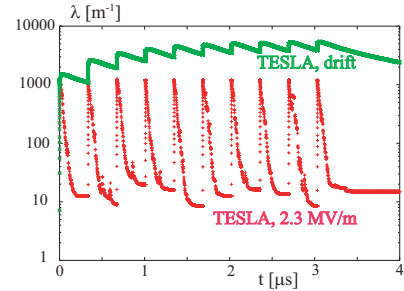
Figure 3: Evolution of electron line density during the passage of 10 bunches for TESLA without rf and with an rf field 10 times smaller than nominal.

Figures 3 and 4 display preliminary simulation results for a maximum secondary emission yield of $\delta_{\mathrm{max}} = 1.7$. Figure 3 shows that a weak rf field suppresses the electron build up which is present without rf. In Fig. 4 a higher rf field causes a linear increase in electron number along the bunch train. Figure 5 presents the energy of the electrons hitting the wall for the same two rf fields as in Fig. 4. Electrons acquire energies of several keV or 10s of keV. Most of the electrons hit the wall close to the horizontal plane, which is a reflection of the pinch inside the bunch field and the large vertical disruption. The electron distribution in the horizontal-longitudinal plane at the end of the last bunch passage is shown in Fig. 6 for GLC/NLC with the nominal rf gradient. The figure reveals that electrons are concentrated inside the beam and at the wall. An accumulation of electrons is visible also near the left iris. Interestingly, at 10 times higher gradient (not shown), electrons impact primarily on the right iris, presumably due to the higher efficiency of acceleration towards the right, i.e., in beam direction. An electron trajectory for this case

is shown in Fig. 7. Initially the electron is accelerated in the direction opposite to the positron beam motion, but at a later time it slows down and starts moving towards the right. The longitudinal turning point coincides with a moment of fast acceleration in the transverse direction.
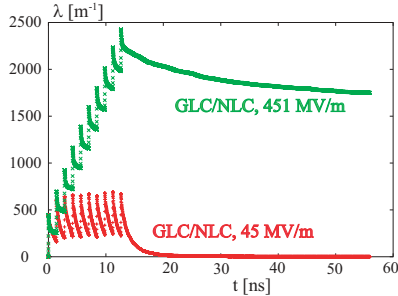
Figure 4: Evolution of electron line density during the passage of 10 bunches followed by a gap for GLC/NLC with nominal and 10 times higher rf gradient.
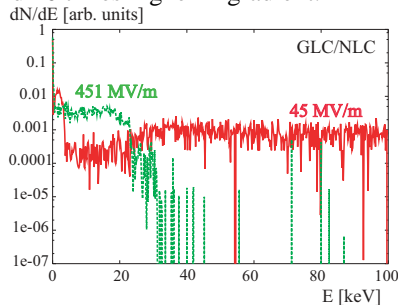
Figure 5: Energy distribution of electrons hitting the cell wall in GLC/NLC for two rf gradients.
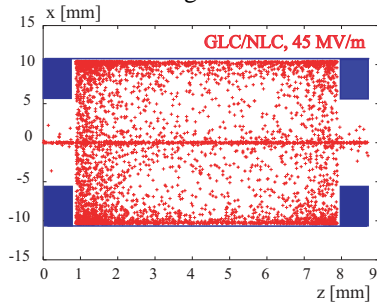
Figure 6: Snapshot of electron $z - x$ distribution after the last bunch passage for GLC/NLC at nominal rf gradient.

CONSEQUENCES

If electrons are present near the beam, they can drive beam instabilities, change the single-particle optics, and cause particle losses by scattering.

We can estimate the beam break-up instability driven by ionization electrons from a two-particle model with acceleration. Taking the electron wake field acting on the trailing particle from [5], assuming that the beta function along the linac grows as $\sqrt{\gamma}$, and modifying the treatment of [6] to account for the increase of the wake (beam-size decrease) along the linac, we estimate the beam break up parameter $\Upsilon_{\text{BBU}} \approx 2\pi\rho_{e,i}r_e L\beta_i/\gamma_i^{3/2}$, where the subindex i refers to quantities at the start of the linac, and $\rho_{e,i}$ is the electron volume density generated by the leading half of the bunch, which amounts to 7×10^{10} m^{-3}, 2×10^{11} m^{-3}, and 1.4×10^{12} m^{-3}, for TESLA, NLC/GLC and CLIC, respectively. The parameter Υ, describing the enhancement
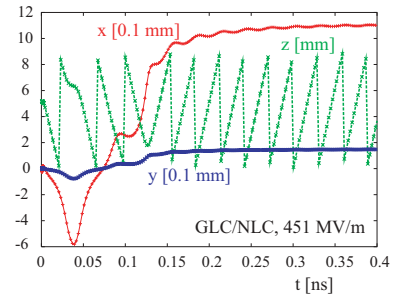
Figure 7: Sample trajectory, showing the horizontal, vertical, and longitudinal motion of an electron for GLC/NLC at an rf gradient equal to 10 times the nominal.

of an oscillation at the bunch tail, is of the order 10^{-3}, if the only electrons present are those due to collisional ionization. Hence, the beam break up is weak in this case.

The focusing effect of a uniform electron cloud inside the bunch is described by $\Delta\phi(L) = 2\pi r_e\rho_e\beta L/\gamma$. Since $\rho_e \propto \gamma/\beta$, if the electron creation is solely due to collisional ionization, the right-hand side does not depend on the beam energy, and, in this case, we have $\Delta\phi(L)^{\text{ion}} \approx r_e N_b\sigma_{\text{ion}}/(\sqrt{\epsilon_x\epsilon_y})(p/(k_BT))L$, which amounts to 5°, 2°, and 6° phase shift for a length of 10 km in the TESLA, GLC/NLC and CLIC linacs, respectively. With field ionization also present, the phase shift could exceed 360°.

The probability for scattering of beam positrons off individual electrons was estimated to be negligible.

CONCLUSIONS

At elevated vacuum pressure, collisional ionization can lead to electron densities which degrade the beam quality. For high beam energies, also field ionization becomes important, supplying a larger number of electrons. Rf fields have a profound influence on the electron dynamics: moderate fields can suppress the build up; higher rf gradients trap or accelerate the primary electrons, which may acquire energies up to 10s or 100s of keV. The simulation of the electron dynamics in strong high-frequency fields requires special care in the choice of integration steps. Our simulation model is only approximate and should be reviewed in future work. Without multipacting, the possibility of beam-break up due to ionization electrons appears remote, thanks to rapid acceleration. Also, though focusing errors between several and 360 degrees may occcur along the length of the linac, and be different from bunch to bunch, the resulting emittance growth is small, roughly equivalent to that caused by a momentum error of a few permille. Incoherent scattering off electrons is negligible. In electron linacs, the fast beam-ion instability [7] may be a limitation.

REFERENCES

[1] T. Raubenheimer and P. Chen, Linac'92, Ottawa (1992).

[2] P.B. Corkum, Phys. Rev. Letters 62, 11 (1989).

[3] A. Murokh, PAC 2003 Portland (2003).

[4] S.D. Ganichev et al., Phys. Rev. Lett. 80, 11, p. 2409 (1998).

[5] K. Ohmi, F. Zimmermann, PRL 85, 3821 (2000).

[6] F. Zimmermann, JAS'2000, CERN-SL-2000-069 (AP).

[7] T. Raubenheimer, F. Zimmermann, PRE 52, 5499 (1995).